DALTON
FULL PAPER

New multidentate ligands for supramolecular coordination chemistry: double and triple helical complexes of ligands containing pyridyl and thiazolyl donor units

Craig R. Rice,*[a] Stefan Wörl,[b] John C. Jeffery,[b] Rowena L. Paul[b] and Michael D. Ward †[b]

[a] *Department of Chemical and Biological Sciences, University of Huddersfield, Huddersfield, UK HD1 3DH. E-mail: c.r.rice@hud.ac.uk*
[b] *School of Chemistry, University of Bristol, Cantock's Close, Bristol, UK BS8 1TS*

Received 2nd October 2000, Accepted 11th January 2001
First published as an Advance Article on the web 15th February 2001

Four new multidentate N-donor ligands L^1–L^4 have been prepared which contain a combination of pyridyl and thiazolyl donor units. The syntheses of these ligands are facile and high-yielding, being based on reaction of an α-bromoacetyl unit with a thioamide to form the thiazolyl ring. The extended linear sequence of *ortho*-linked N-donor heterocycles (four for L^1, six for L^2; five for L^3; and six for L^4) is reminiscent of the well-known linear oligopyridines, although these new ligands are much easier to make and have significantly different geometric coordination properties because the presence of the five-membered thiazolyl rings results in natural breaks of the ligand backbone into distinct bidentate or terdentate domains. Thus, the tetradentate ligand L^1 partitions into two bidentate domains to give dinuclear triple helicates $[M_2(L^1)_3]^{4+}$ with six-coordinate first-row transition metal dications (M = Co, Cu, Zn). The hexadentate ligand L^2 partitions into two terdentate domains to give dinuclear double helicates $[M_2(L^2)_2]^{4+}$ with six-coordinate metal ions (M = Cu, Zn). In the double helicate $[Cu_2(L^3)_2]^{4+}$ the pentadentate ligand L^3 only uses its two terminal bidentate binding sites, resulting in four-coordinate Cu(II) centres and a non-coordinated pyridyl residue in the centre of each of the two ligand strands. These pendant pyridyl residues are directed towards each other to give a potentially two-coordinate cavity between the metal ions in the centre of the helicate. Similarly, in the double helicate $[Cu_2(L^4)_2]^{4+}$ the metal ions are only four-coordinate, with each ligand having its central bipyridyl unit un-coordinated. This results in a potentially four-coordinate cavity between the two metal ions in the centre of the helicate. These easy-to-prepare ligands offer a great deal of scope for the development of multinuclear helicates.

Introduction

Studies on the assembly of double and triple helicate complexes have been a major area of activity in coordination chemistry for the last 15 years or so. These assemblies have elegantly demonstrated how the formation of architecturally complex systems is directed by the interplay between simple parameters such as the stereoelectronic preference of the metals ion and the disposition of the binding sites in the ligand.[1]

A key parameter in the assembly of helicates is how a flexible polydentate ligand becomes partitioned into distinct metal binding sites. In many cases ligands have been constructed which contain several bidentate or terdentate domains which are so arranged that each site must necessarily bind a separate metal ion rather than chelating to a single metal ion — a necessary prerequisite for helication. Ligands of this type are exemplified by the recent work of Albrecht *et al.*,[2] Piguet and co-workers[3] and Lehn and co-workers[4] amongst others.[5] In other cases however, most notably the linear polypyridines which have played a major role in the development of helicates,[6,7] the way in which the ligand is partitioned into binding sites depends on the stereoelectronic preferences of the metal ion which become all-important in directing the course of the assembly. Thus, 2,2′ : 6′,2′ : 6′,2‴-quaterpyridine (qpy) acts as a planar tetradentate chelate to first-row transition-metal dications, as well as to Pd(II) and Pt(II);[8,9] but it acts as a 2 + 2 bridging ligand (two independent bipyridyl units) to Ag(I) and Cu(I) in the dinuclear double helicates $[M_2(qpy)_2]^{2+}$ whose assembly is driven by the preference of the metal ions for pseudo-tetrahedral geometry.[9] Similarly, the hexadentate ligand 2,2′ : 6′,2′ : 6′,2‴ : 6‴,2⁗ : 6⁗,2′-sexipyridine (spy) can be partitioned into two terdentate or three bidentate binding domains according to whether the metal ion prefers octahedral [Cd(II)] or tetrahedral coordination [Cu(I)].[10]

We describe in this paper the synthesis and coordination chemistry of a series of polydentate *N*-donor ligands based on pyridyl and thiazolyl donors. These may be considered as analogues of the well-known polypyridines, but with two important exceptions. Firstly, the incorporation of five-membered thiazole units into the chain results in a natural partition of the ligand into separate binding domains. The coordination behaviour of these ligands can therefore be controlled according to the position of the thiazole units in the chain. Secondly, these ligands are exceptionally easy to prepare in high yields using a simple modular approach; syntheses of these ligands and their intermediates does not require chromatographic purification at any stage. This paper reports the syntheses of four new ligands and the structures of several of their double- or triple-helical complexes with first-row transition-metal ions. A preliminary communication describing some of these results has appeared recently.[11] We note that thiazole units have also been incorporated into other polydentate ligands by Connor and co-workers, who previously prepared one of the ligands described in this paper (L^4) but did not describe any of its coordination chemistry.[12]

Results and discussion

Ligand syntheses

The ligands described are shown in Scheme 1. The key step in

† Royal Society of Chemistry Sir Edward Frankland fellow for 2000/2001.

 DOI: 10.1039/b007922g

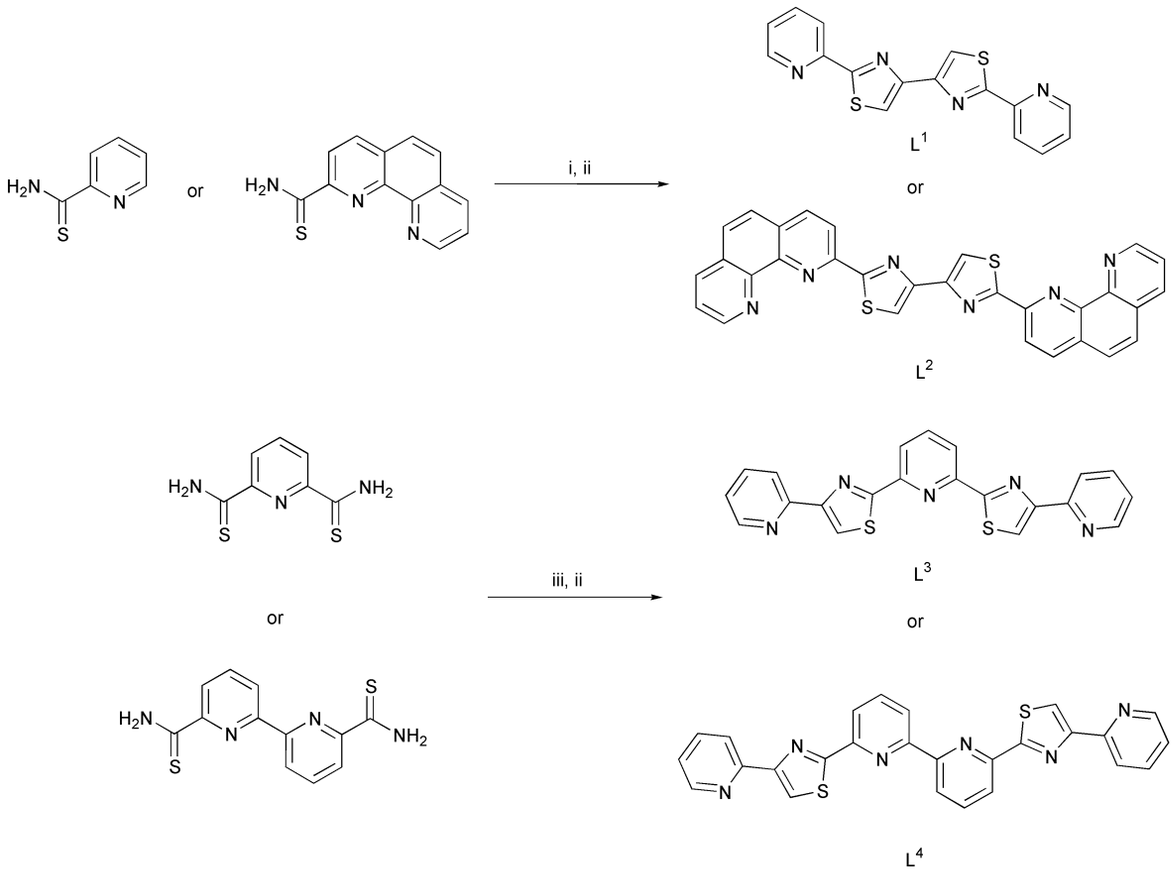

Scheme 1 Reagents and conditions: i, $(COCH_2Br)_2$, MeOH; ii, NH_3(aq); iii, 2-(α-bromoacetyl)pyridine, MeOH.

every synthesis is assembly of the thiazole unit from reaction of an α-bromoacetyl group with a thioamide. The α-bromoacetyl group is simply prepared by bromination of an acetyl group,[13] and the thioamide is equally simply prepared by reaction of a cyano group with H_2S.[12,14] Using this methodology allows, in principle, the preparation of a very wide variety of related ligands, as long as components bearing acetyl or cyano substituents are available as starting materials.

Thus, L^1 was prepared by reaction of two equivalents of pyridine-2-thioamide with 1,4-dibromobutane-2,3-dione in methanol at reflux. After 1 hour L^1 precipitates cleanly as its hydrobromide salt, from which free L^1 is obtained quantitatively by deprotonation with ammonia. Following the same method, L^2 was prepared from reaction of 1,10-phenanthroline-2-thioamide with 1,4-dibromobutane-2,3-dione. Pentadentate L^3 was prepared from pyridine-2,6-di(thioamide) with 2-(α-bromoacetyl)pyridine, and the potentially hexadentate ligand L^4 was prepared in the same way as L^3 but using 2,2′-bipyridine-6,6′-di(thioamide). In all cases the ligands were isolated in high yield as crystalline solids which were sufficiently pure to be used for formation of metal complexes without further purification, although samples for analysis were recrystallised. All of the ligands gave correct elemental analyses and showed the expected molecular ion in their EI mass spectra. L^1, L^2 (as the hydrobromide salt), L^3 and L^4 were further characterised by ^{1}H NMR spectroscopy (see the Experimental section).

The crystal structure of L^1 (Fig. 1) shows the molecule to be essentially planar, with an all-*transoid* geometry between the N atoms of adjacent heterocyclic rings. In this respect the structure is similar to those of the linear polypyridine ligands.[15] The molecules are arranged in canted stacks in the crystal with separations between adjacent molecules (defined as the distance from an atom in one molecule to the mean plane of the next molecule) lying between 3.3 and 3.6 Å, which is normal for aromatic π-stacking interactions. In addition, between

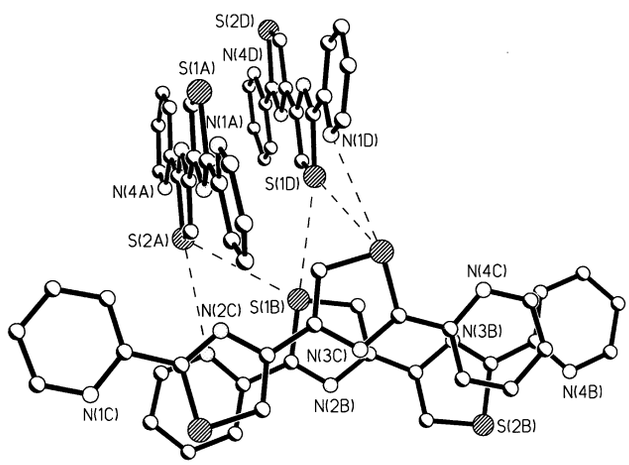

Fig. 1 Crystal structure of L^1 emphasising the intermolecular interactions. Bond lengths and angles within the molecule are unremarkable.

adjacent stacks there are non-bonded S ··· S interactions [S(1) ··· S(1′), 3.475 Å; S(1) ··· S(2′), 3.605 Å] and S ··· N interactions [N(1) ··· S(2′), 3.276 Å] involving thiazole S and pyridyl N atoms (Fig. 1). Such interactions are well known and arise from interaction of the lone pair of the donor unit (N or S) with a C–S(σ*) orbital from the acceptor unit (always S);[16] clearly these interactions exert a strong influence on the crystal packing in this case.

Dinuclear triple helicates with L^1

Although L^1 is poorly soluble in common organic solvents, it dissolves quickly on coordination to a metal ion to give soluble complexes. Reaction of L^1 with $Co(ClO_4)_2$ or $Zn(ClO_4)_2$ (in nitromethane) or $Cu(PF_6)_2$ (in acetone) in a 3 : 2 ratio rapidly afforded clear solutions of complexes, from which a good yield

Table 1 Crystallographic data[a]

Compound	L^1	$[Cu_2(L^1)_3][PF_6]_4\cdot 4Me_2CO$	$[Zn_2(L^1)_3][ClO_4]_4\cdot 4MeNO_2$	$[Co_2(L^1)_3][ClO_4]_4\cdot 4MeNO_2$	$[Co_2(L^2)_2][ClO_4]_4\cdot 8MeCN\cdot H_2O$	$[Zn_2(L^2)_2][ClO_4]_4\cdot 9MeCN$	$[Cu_2(L^3)_2][ClO_4]_4\cdot 4MeNO_2$	$[Cu_2(L^4)_2][ClO_4]_4\cdot 2MeNO_2$
Formula	$C_{16}H_{10}N_4S_2$	$C_{60}H_{54}Cu_2F_{24}N_{12}O_4P_4S_6$	$C_{52}H_{42}Cl_4N_{16}O_{24}S_6Zn_2$	$C_{52}H_{42}Cl_4Co_2N_{16}O_{24}S_6$	$C_{76}H_{58}Cl_4Cu_2N_{20}O_{17}S_4$	$C_{78}H_{59}Cl_4N_{21}O_{16}S_4Zn_2$	$C_{46}H_{38}Cl_4Cu_2N_{14}O_{24}S_4$	$C_{54}H_{38}Cl_4Cu_2N_{14}O_{20}S_4$
M	322.4	1906.5	1739.9	1727.0	1920.5	1947.2	1568.0	1600.1
T/K	173	173	173	173	173	123	173	173
System, space group	Orthorhombic, *Pbcn*	Monoclinic, *C*2/*c*	Monoclinic, *C*2/*c*	Monoclinic, *C*2/*c*	Triclinic, $P\bar{1}$	Triclinic, $P\bar{1}$	Triclinic, $P\bar{1}$	Triclinic, $P\bar{1}$
a/Å	11.882(5)	13.9497(14)	13.329(3)	13.2594(7)	13.4641(13)	13.430(5)	12.0704(17)	12.4345(6)
b/Å	9.871(4)	23.133(2)	23.158(3)	23.1248(12)	15.0528(15)	15.088(6)	13.675(2)	12.5367(6)
c/Å	24.086(10)	22.485(2)	22.379(3)	22.4373(11)	21.859(2)	21.650(8)	19.688(3)	20.9227(11)
α/°					80.685(2)	81.050(7)	94.440(3)	89.8910(10)
β/°		99.792(2)	99.357(19)	99.8610(10)	81.242(2)	80.641(8)	104.884(3)	76.8420(10)
γ/°					77.288(2)	78.684(8)	106.271(3)	79.2060(10)
U/Å^3	2825(2)	7150.3(12)	6815.9(19)	6778.1(6)	4233.1(7)	4210(3)	2975.5(7)	3116.9(3)
Z	8	4	4	4	2	2	2	2
μ/mm^{-1}	0.377	0.980	1.135	0.923	0.806	0.875	1.130	1.076
Reflections collected: total, independent, R_{int}	11085, 1851, 0.182	19016, 6291, 0.100	21828, 7794, 0.0251	21778, 7757, 0.0317	22820, 7887, 0.1418	22584, 7859, 0.1585	31484, 13557, 0.0885	32873, 14162, 0.0474
Final $R1$, $wR2$ [b,c]	0.0941, 0.2307	0.0886, 0.2807	0.0772, 0.2630	0.1011, 0.3315	0.0984, 0.2884	0.1594, 0.4198	0.0727, 0.2080	0.0570, 0.1675

[a] Details in common: diffractometer, Siemens SMART using Mo-Kα radiation (0.71073 Å). [b] The structure was refined on F_o^2 using all data; the value of $R1$ is given for comparison with older refinements based on F_o with a typical threshold of $F \geq 4\sigma(F)$. [c] $wR2 = [\Sigma[w(F_o^2 - F_c^2)^2]/\Sigma w(F_o^2)^2]^{1/2}$ where $w^{-1} = [\sigma^2(F_o^2) + (aP)^2 + bP]$ and $P = [\max(F_o^2, 0) + 2F_c^2]/3$.

Table 2 Selected bond distances (Å) and angles (°) for complexes $[Cu_2(L^1)_3][PF_6]_4\cdot 4Me_2CO$, $[Co_2(L^1)_3][ClO_4]_4\cdot 4MeNO_2$ and $[Zn_2(L^1)_3][ClO_4]_4\cdot 4MeNO_2$

	M = Co	M = Cu	M = Zn
M–N(21)	2.130(5)	2.028(8)	2.150(4)
M–N(31)	2.150(5)	2.056(7)	2.198(4)
M–N(61A)	2.182(6)	2.171(8)	2.194(4)
M–N(11)	2.161(5)	2.187(8)	2.195(4)
M–N(41)	2.138(6)	2.192(8)	2.164(5)
M–N(51A)	2.143(5)	2.219(8)	2.168(4)
N(21)–M–N(31)	172.7(2)	171.5(3)	171.94(16)
N(21)–M–N(61A)	98.4(2)	96.7(3)	98.60(18)
N(31)–M–N(61A)	83.6(2)	87.2(3)	84.46(16)
N(21)–M–N(11)	77.7(2)	79.2(3)	78.05(17)
N(31)–M–N(11)	100.6(2)	97.1(3)	99.40(15)
N(61A)–M–N(11)	175.1(2)	175.4(3)	174.74(15)
N(21)–M–N(41)	95.4(2)	92.9(3)	95.07(17)
N(31)–M–N(41)	77.3(2)	79.1(3)	77.08(15)
N(61A)–M–N(41)	98.5(3)	97.8(3)	98.22(19)
N(11)–M–N(41)	85.0(2)	84.8(3)	86.18(17)
N(21)–M–N(51A)	86.9(2)	86.8(3)	88.58(16)
N(31)–M–N(51A)	100.40(18)	101.4(3)	99.39(14)
N(61A)–M–N(51A)	76.9(2)	76.8(3)	76.81(15)
N(11)–M–N(51A)	99.74(18)	100.5(3)	98.94(14)
N(41)–M–N(51A)	175.1(2)	174.5(3)	174.25(15)

of crystalline product could be isolated in each case by diffusion of ethyl acetate vapour into the solution. In each case, electrospray mass spectroscopy and elemental analyses indicated formation of a complex of the form $[M_2(L^1)_3]X_4$. The ^{1}H NMR spectrum of $[Zn_2(L^1)_3][ClO_4]_4$ in CD_3NO_2 showed the presence of just five resonances in the aromatic region of the spectrum [Fig. 2(a)] (of which two are overlapping), indicating that all six pyridyl–thiazolyl units are equivalent in solution on the NMR timescale, which is only consistent with all three ligands adopting a symmetrically bridging coordination mode. This was confirmed by determination of the crystal structures of all three complexes (see Tables 1 and 2).

All three complexes are dinuclear triple helicates and the structures are very similar to one another (Figs. 3 and 4). In each complex, both metal centres have a pseudo-octahedral coordination geometry arising from coordination of three thiazolyl–pyridyl bidentate units. To accommodate this bridging coordination mode, each ligand L^1 is twisted about the bond between the two thiazole rings (torsion angles in the range 58° to 79°) such that each ligand can present a bidentate binding site to each metal ion without steric problems. The triple helical structure is stabilised by extensive aromatic π-stacking interactions between overlapping, near-parallel fragments of adjacent ligands, as emphasised in the space-filling picture (Fig. 4). Details of the relevant structural parameters for each complex are summarised in Table 2, with parameters that are equivalent between structures positioned in the same row of the table to facilitate comparison.

The only significant difference between the structures is in the degree of distortion in the metal coordination spheres. Whereas the Co(II) and Zn(II) complexes have a relatively narrow range of M–N separations [2.13–2.18 Å for Co(II); 2.15–2.20 Å for Zn(II)], for the Cu(II) complex the bond distances lie between 2.03–2.22 Å, a spread of *ca.* 10%. This is undoubtedly due to the Jahn–Teller effect: although there is no single obvious axis of elongation as usually occurs in complexes of tetragonal symmetry, the distortion manifests itself in one axis [N(21)–Cu–(31) axis, average Cu–N distance 2.04 Å] being significantly shorter than the other two [N(11)–Cu–N(61A), average Cu–N distance 2.18 Å; and N(41)–Cu–N(51A), average Cu–N distance 2.21 Å]. This apparent axial compression has been ascribed to a dynamic Jahn–Teller effect in which a *single* axis of elongation — the electronically most likely distortion — is disordered over two axes.[17] In this case it is clear from the

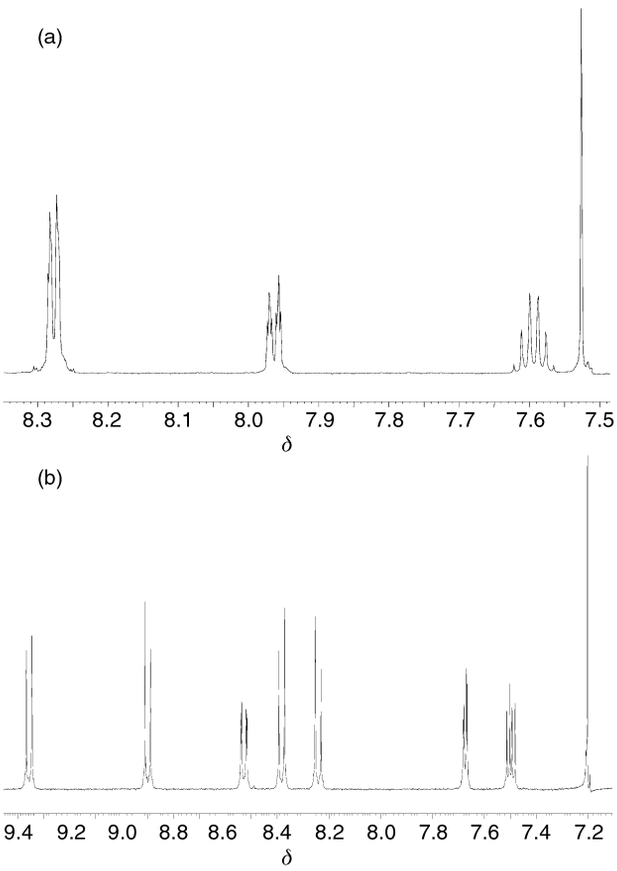

Fig. 2 ^{1}H NMR spectra of (a) the triple helicate $[Zn_2(L^1)_3][ClO_4]_4$, and (b) the double helicate $[Zn_2(L^2)_2][ClO_4]_4$ ($MeNO_2$, 300 MHz).

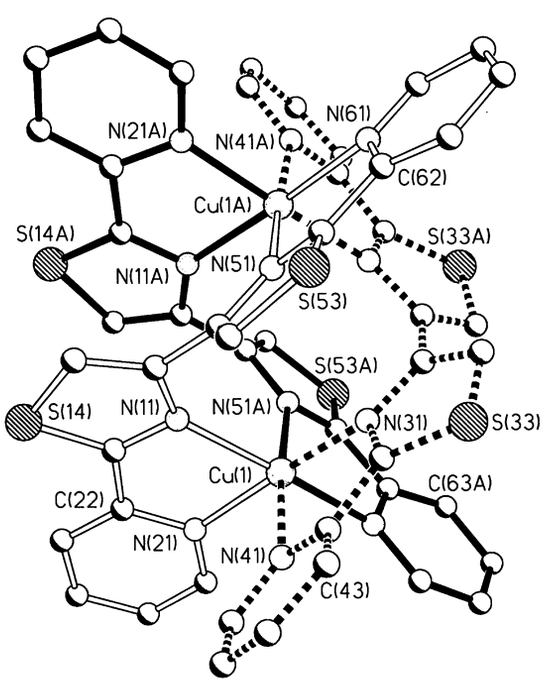

Fig. 3 Crystal structure of the complex cation of $[Cu_2(L^1)_3][ClO_4]_4$ [the structures of the Co(II) and Zn(II) analogues are essentially identical apart from minor changes in bond lengths/angles in the metal coordination sphere].

comparison between the distorted Cu(II) complex, and the more regular Co(II) and Zn(II) complexes, that the structural distortion of $[Cu_2(L^1)_3]^{4+}$ arises from a genuine stereoelectronic preference of the metal ion, rather than being imposed by the ligand.

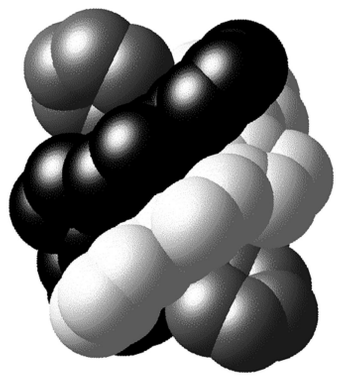

Fig. 4 Space-filling picture of the triple helical complex cation of $[Zn_2(L^1)_3][PF_6]_4$.

The formation of triple helicates with L^1 is in interesting contrast to the many mononuclear complexes in which qpy acts as a simple equatorial tetradentate chelate to a +2 metal ion.[8] In qpy this coordination mode is facilitated by the fact that all three chelate rings have a bite angle appropriate for coordination to a single metal ion. In L^1 this is not the case; the two five-membered thiazolyl rings cannot chelate well because the N atoms of the two five-membered rings are not sufficiently convergent, so the ligand naturally partitions into two bidentate pyridyl–thiazolyl units with a twist in the ligand backbone between them. The result is a dinuclear triple helicate instead of a simple mononuclear complex.

Dinuclear double helicates with L^2

Given the way that L^1 was observed to behave, we might expect that L^2 partitions into two terdentate domains with the break occurring between the two thiazolyl rings. Reaction of L^2 with $Cu(ClO_4)_2$ or $Zn(ClO_4)_2$ afforded complexes for which the elemental analyses were consistent with the empirical formulation $[M(L^2)](ClO_4)_2$; electrospray mass spectra indicated the formation of dimeric complex cations $[M_2(L^2)_2]^{4+}$ (M = Cu, Zn). The ^{1}H NMR spectrum of the Zn(II) complex [Fig. 2(b)] shows the presence of eight aromatic proton environments, indicating a high-symmetry structure in which all four ligand halves are chemically equivalent.

The crystal structures of both complexes reveal that they are dinuclear double helicates, with each metal ion being six-coordinate from two terdentate fragments, one from each of the two ligands (Figs. 5 and 6). The bridging coordination mode of each ligand is facilitated by a twist of *ca.* 90° between the two thiazolyl rings. In $[Cu_2(L^2)_2]^{4+}$ (Fig. 5) the two metal centres are in a very irregular coordination environment, but it is nonetheless clear that one of the axes is substantially shorter than the other two at each metal centre. For Cu(1), the N(144)–Cu(1)–N(121) axis (average Cu–N distance, 1.98 Å) is shorter than the N(101)–Cu(1)–N(141) and N(111)–Cu(1)–N(124) axes (average Cu–N distances, 2.23 and 2.17 Å respectively). For Cu(2), the N(244)–Cu(2)–N(221) axis (average Cu–N distance, 1.97 Å) is shorter than the N(201)–Cu(1)–N(241) and N(211)–Cu(1)–N(224) axes (average Cu–N distances, 2.22 and 2.23 Å respectively). As with any Cu(II) complex in a constrained geometry it is not easy to know to what extent this distortion is due to the Jahn–Teller effect, and to what extent it is imposed by the ligand set, however comparison with the Zn(II) complex provides some clues. In fact, the crystal structure of the Zn(II) double helicate $[Zn_2(L^2)_2]^{4+}$ also shows a similar pattern with one axis having shorter bond lengths than the other two. For Zn(1), the N(141)–Zn(1)–N(124) axis has a mean Zn–N distance of 2.07 Å; for the axes N(111)–Zn(1)–N(121) and N(101)–Zn(1)–N(144) the mean Zn–N distances are 2.20 and 2.21 Å respectively. Around Zn(2), the short axis is N(221)–Zn(2)–N(244), with a mean Zn–N distance of 2.05 Å; for the

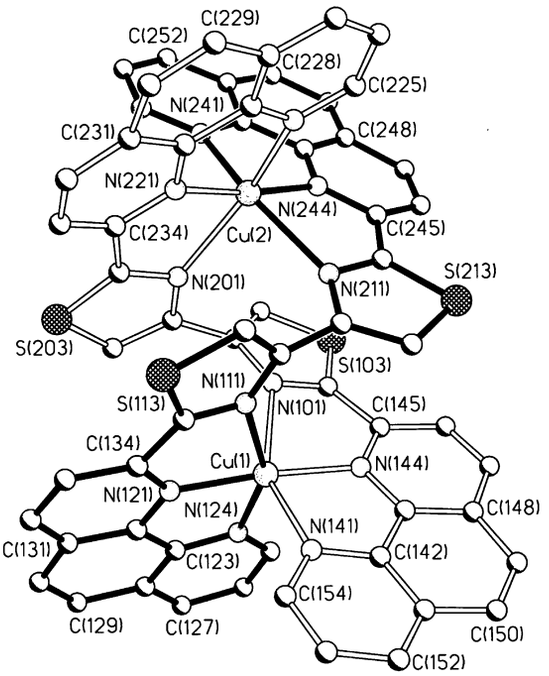

Fig. 5 Crystal structure of the complex cation of $[Cu_2(L^2)_2][ClO_4]_4$ [the structure of the Zn(II) analogue is essentially identical apart from minor changes in bond lengths/angles in the metal coordination sphere].

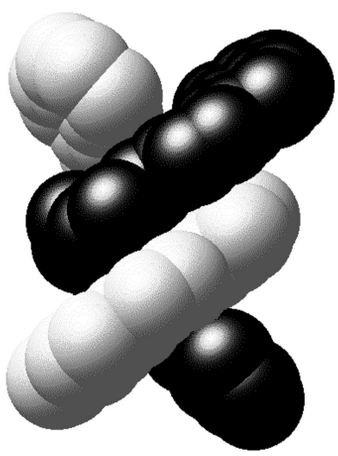

Fig. 6 Space-filling picture of the double helical complex cation of $[Zn_2(L^2)_2][ClO_4]_4$.

axes N(211)–Zn(2)–N(241) and N(201)–Zn(2)–N(224) the mean Zn–N distances are 2.23 and 2.19 Å respectively. These differences are sufficiently large to be significant even considering the poor quality of the structure of the Zn complex.

The pattern of metal–ligand bond lengths in $[Zn_2(L^2)_2]^{4+}$ therefore matches well that seen for $[Cu_2(L^2)_2]^{4+}$, although the difference in length between the one short and the two long axes is more pronounced for the Cu(II) complex. This suggests that the coordination geometry is largely imposed by the ligand set, and is less easily ascribed to stereoelectronic effects — in direct contrast to the behaviour of the triple helicates with L^1 (see above). In every case the short axis is the one with two bonds to the central donor atom of each terdentate unit. We are therefore seeing a structural distortion of the type typical of terpyridyl complexes, where the M–N distance to the central pyridyl ring is significantly shorter than the bonds to the two terminal pyridyl rings.[18] This is a consequence of the fact that the natural bite angle of terpyridine, which is 120°, is mis-matched with the usual preference of the metal centre for a bite angle of 180° from a terdentate chelate, and similar geometric behaviour is shown by the thiazolyl–phenanthroline unit of L^2.

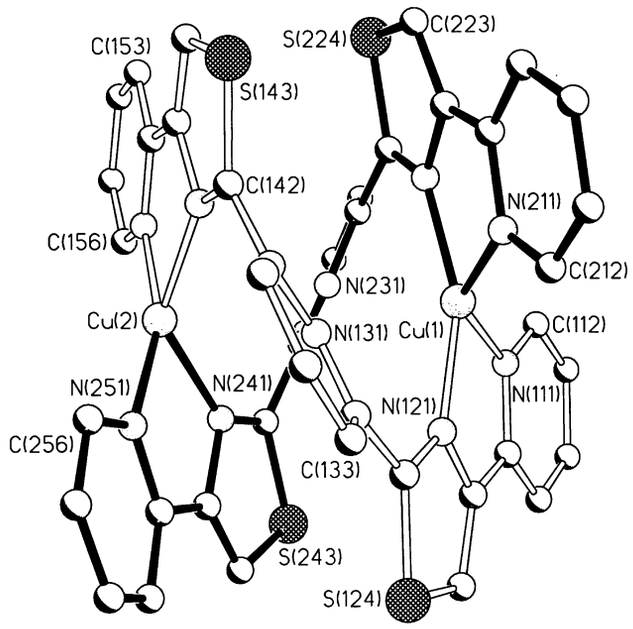

Fig. 7 Crystal structure of the complex cation of $[Cu_2(L^3)_2][ClO_4]_4$.

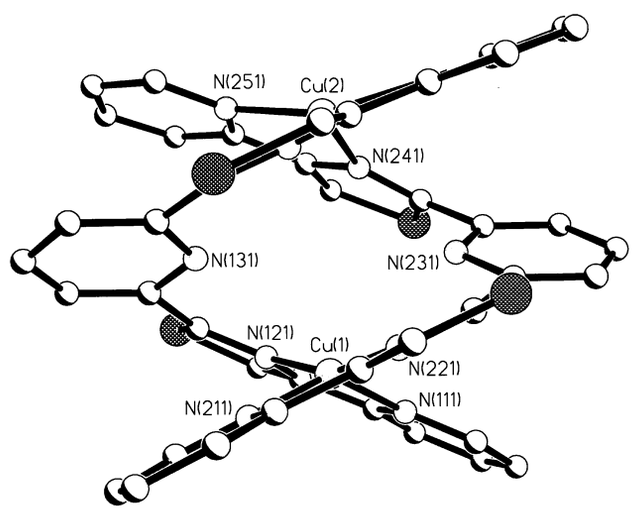

Fig. 8 Alternative view of the complex cation $[Cu_2(L^3)_2]^{4+}$, emphasising the two-coordinate cavity at the centre of the helicate.

Dinuclear double helicates with L^3 and L^4 showing hypodentate coordination

The potentially pentadentate ligand L^3 contains thiazolyl units at positions 2 and 4 of the five-ring sequence. Whilst a bidentate pyridyl–thiazolyl fragment can clearly act as an effective bidentate chelate (*cf.* complexes with L^1), simple molecular modelling suggests that a terdentate pyridyl–thiazolyl–pyridyl unit — with the five-membered thiazolyl ring in the centre — cannot easily act as a terdentate chelate as the two terminal pyridyl units are not sufficiently convergent. The way in which L^3 could be partitioned into separate binding domains is therefore not as clear as it is for L^1 and L^2: there are several ways in which two bidentate pyridyl–thiazolyl fragments can be donated to metal ions, but these will all result in a spare pyridyl donor (hypodentate coordination of the ligand).[6]

This behaviour is illustrated by the crystal structure of $[Cu_2(L^3)_2][ClO_4]_4$, (Figs. 7 and 8) which was prepared by reaction of $Cu(ClO_4)_2$ with L^3, in the same manner as for the earlier complexes. The complex cation is again a double helicate, with two four-coordinate Cu ions each coordinated by two bidentate pyridyl–thiazolyl units, one from the terminus of each ligand. The result of this is that the central pyridyl residue of each ligand is not coordinated, but just acts as an innocent spacer

group separating the two bidentate binding sites. Across the centre of the complex, the non-bonded N ··· N separation between the two non-coordinated pyridyl residues is 4.36 Å. The geometry about the two Cu(II) ions is of the type generally described as pseudo-tetrahedral, although the two bidentate fragments at each metal centre are not mutually perpendicular. At Cu(1) the dihedral angle θ between the two Cu(NN) planes is 47.5°, so the geometry is almost mid-way between planar (D_{2h} local symmetry of the CuN_4 unit, arising from $\theta = 0°$ between the two CuNN planes) and tetrahedral (D_{2d} local symmetry of the CuN_4 unit, arising from $\theta = 90°$ between the two CuNN planes). At Cu(2) this dihedral angle θ is 49.7°. In addition, there is extensive aromatic π-stacking between overlapping, near-parallel segments of the two ligands with average interplanar distances in the region of 3.5–3.7 Å. The Cu ··· Cu separation is 4.325 Å.

It is interesting to note that the irregular four-coordinate geometry, and the range of Cu–N bond distances (1.97–2.07 Å), are also typical of Cu(I) centres with NN-chelating ligands such as derivatives of bipyridine and phenanthroline.[19] From the crystal structure alone it is not obvious whether the oxidation state of the metal is +2 or +1, although we note that for $Cu^{I}(NN)_2$ complexes the value of θ is usually 70–80°,[19] compared to 45–50° in this helicate which is more suggestive of Cu(II). Although there are four counter-ions, it is in principle possible that the pendant pyridyl units could be protonated such that the four positive charges are provided by two Cu(I) centres and two protons. The ambiguity is simply resolved by the electronic spectrum of the complex in $MeNO_2$, which reveals a transition at $\lambda_{max} = 706$ nm (ε *ca.* 300 M^{-1} cm^{-1}) with a low-energy shoulder at around 900 nm. This is entirely characteristic of Cu(II) in an irregular coordination environment, for which up to four d–d transitions may be expected, although usually only one or two are resolved due to their width and the close spacing of the individual maxima.[20] In addition, an EPR spectrum of the complex in $MeNO_2$ solution confirmed that is paramagnetic with a broad transition centred at $g = 2.14$; in a frozen solution at 77 K the spectrum remained broad and poorly resolved with only a single feature present at $g = 2.12$. These spectra are indicative of weak Cu–Cu magnetic exchange which broadens the signal to an extent which precludes any geometric analysis of the results, but the presence of a strong signal in this position confirms the oxidation state assigment as Cu(II).

The crystal structure of $[Cu_2(L^4)_2][ClO_4]_4$ (Figs. 9 and 10) shows similar hypodentate behaviour with only the terminal bidentate pyridyl–thiazolyl units coordinated to the metal ions and consequently a central non-coordinated bipyridyl fragment. In principle, given that this ligand can partition itself into three potentially bidentate compartments, we might expect a trinuclear double helicate with all three bidentate sites occupied. We could not however isolate such a complex even using an excess of the metal ion in the complexation reaction. Such a structure appears to be disfavoured, possibly because of the electrostatic barrier to having three dipositive metal ions so close together; the Cu ··· Cu separation in this dinuclear helicate is 4.746 Å, and insertion of an additional metal ion between them would result in unrealistically short metal–metal separations. In addition, the helical ligand array is facilitated by a substantial twist between the two halves of each ligand such that the central bipyridyl unit of each is not coplanar. The dihedral angle between the pyridyl rings containing N(251) and N(252) is 36.6°, and the dihedral angle in the other bipyridyl fragment is 48.5°. Such a substantial distortion from planarity of the central bipyridyl fragments clearly precludes chelation to a metal ion.

Again, the metal ions are in distorted four-coordinate geometries with the values of θ [the angle between the two Cu(NN) planes at each metal site] being 60.3° for Cu(1) and 59.7° for Cu(2). This does not tell the whole story because the geometry

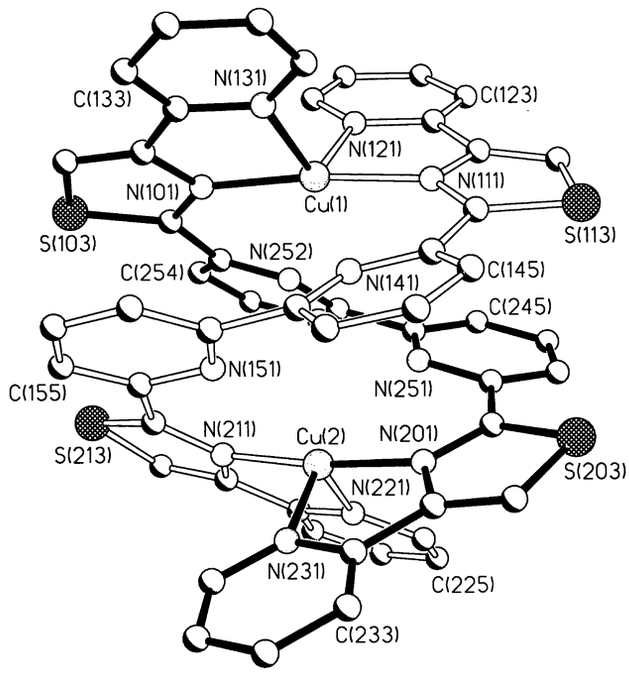

Fig. 9 Crystal structure of the complex cation of $[Cu_2(L^4)_2][ClO_4]_4$.

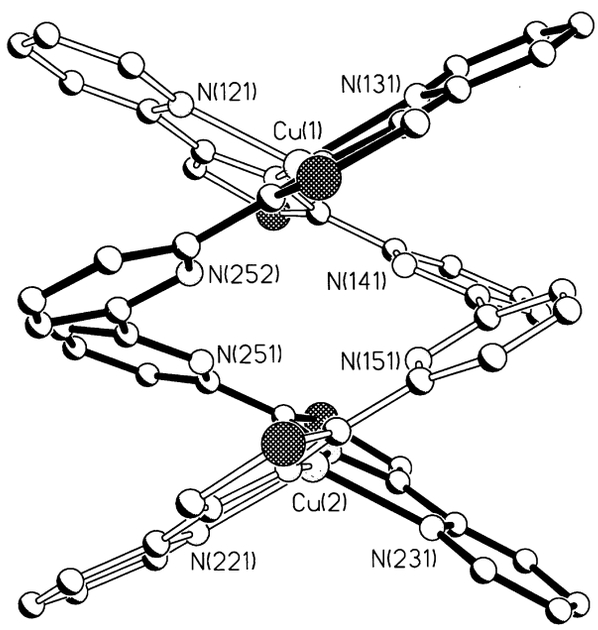

Fig. 10 Alternative view of the complex cation $[Cu_2(L^4)_2]^{4+}$, emphasising the four-coordinate cavity at the centre of the helicate.

about the metal ions, far from being pseudo-tetrahedral (as for the previous complex with L^3), is more like that of an octahedron with a pair of *cis* coordination sites vacant, or a trigonal bipyramid with one equatorial site vacant. The two thiazolyl donors are almost perfectly *trans* to one another, with N–Cu–N angles involving these donors of 173.9 and 173.4° at Cu(1) and Cu(2) respectively. The irregular four-coordinate geometry and the range of Cu–N bond distances (1.92 to 2.14 Å) could, as before, be consistent with Cu(I) and well as Cu(II), but the +2 oxidation state of the metal ions was confirmed by the presence of characteristic d–d transitions at 740 and 1230 nm in the electronic spectrum in $MeNO_2$ (ε *ca.* 200 dm^3 mol^{-1} cm^{-1} in each case).[20] This is in exact agreement with the expectation of two distinct d–d transitions for Cu(II) chromophores with a *cis*-N_4X_2 geometry,[20,21] with the large separation between the transitions reflecting the very high degree of rhombic distortion of the *cis*-CuN_4X_2 chromophore, *i.e.* X = nothing in this case! This strongly suggests that the solid-state structure is retained in

nitromethane solution. Again, EPR analysis in $MeNO_2$ solution allowed confirmation of the oxidation state as Cu(II) with a broad, relatively featureless signal at $g = 2.12$, both at room temperature and at 77 K. The appearance of the spectra as broad and poorly-resolved may again be ascribed to Cu ··· Cu exchange coupling.

An interesting feature of the structures of both $[Cu_2(L^3)_2]^{4+}$ and $[Cu_2(L^4)_2]^{4+}$ is that the non-coordinated fragments in the middle of each ligand (a pyridyl residue in the former case, and a bipyridyl residue in the latter) define a central cavity between the two metal ions. For $[Cu_2(L^3)_2]^{4+}$, with a non-bonded N ··· N separation of 4.36 Å, there is a two-coordinate cavity (Fig. 8) which (steric hindrance apart) could be suitable for binding a guest such as a small molecule with two hydrogen-bond donor sites. In $[Cu_2(L^4)_2]^{4+}$ the cavity is four-coordinate from the two twisted bipyridyl units (Fig. 10), with N ··· N separations between the two bipyridyl fragments across the cavity lying between 3.66 and 4.13 Å. Although binding of an additional metal ion here is likely to be difficult (if not impossible) for the reasons mentioned earlier, the shape and size of the cavity could again be suitable for small-molecule binding *via* hydrogen-bonding with the N atoms acting as the hydrogen-bond acceptors. We note that binding of additional guest species within a helical array has been demonstrated by the groups of Albrecht and Raymond,[22] and similar studies with $[Cu_2(L^3)_2]^{4+}$ and $[Cu_2(L^4)_2]^{4+}$ are in progress.

Although the irregular four-coordinate geometries of the metal centres in $[Cu_2(L^3)_2][ClO_4]_4$ and $[Cu_2(L^4)_2][ClO_4]_4$ suggest that facile interconversion between Cu(II) and Cu(I) might be possible with minimal rearrangement, cyclic voltammetric studies ($MeNO_2$ solvent, Bu_4NPF_6 base electrolyte, Pt working electrode) revealed no reversible electrochemical behaviour, with only irreversible processes at high positive and negative potentials.

Conclusions

The ligands L^1–L^4 are versatile new ligands for the preparation of double and triple helicate complexes with first-row transition-metals. They are exceptionally easy to prepare, in marked contrast to the linear polypyridines that are their most obvious analogues. Their partitioning into bidentate or terdentate binding domains is dependent on the position of the thiazolyl rings in the ligand backbone.

Experimental

General details

The following instrumentation was used for routine spectroscopic measurements: NMR spectra, a JEOL Lambda 300 MHz spectrometer; mass spectra, a VG-Autospec instrument (electron impact) or a VG-Quattro mass spectrometer (electrospray ionisation); electronic spectra, a Perkin-Elmer Lambda 2 spectrometer. EPR spectra were recorded at X-band on a Bruker ESP-3000E spectrometer.

The following compounds were prepared by literature methods: 1,4-dibromobutane-2,3-dione,[13] 1,10-phenanthroline-2-thioamide,[14] 2-(α-bromoacetyl)pyridinium hydrobromide,[13] 2,2′-bipyridine-6,6′-di(thioamide).[12] Starting materials were purchased from the usual commerical sources (Aldrich, Avocado, Lancaster) and used as received.

Preparation of pyridine-2-thioamide

2-Cyanopyridine (10.0 g, 96.0 mmol) was dissolved in a mixture of Et_3N (2 cm^3) and ethanol (30 cm^3). H_2S was slowly bubbled through the solution for 1 h, during which time a yellow precipitate was formed. Collection by filtration gave pure pyridine-2-thioamide as a yellow solid. Yield: 6.63 g, 50%. EI-MS: *m*/*z* 138 (75%, M^+). ^{1}H NMR [300 MHz, $(CD_3)_2SO$]: δ 10.51 (1H, s, NH), 10.24 (1H, s, NH), 8.70 (1H, d, py), 8.31 (1H, d, py), 8.15 (1H, t, py), 7.68 (1H, t, py). Found: C, 52.0; H, 4.4; N, 20.0%; $C_6H_6N_2S$ requires C, 52.1; H, 4.4; N, 20.3%.

Preparation of pyridine-2,6-di(thioamide)

This was prepared in exactly the same way as described for pyridine-2-thioamide, by bubbling H_2S for 1 h through a solution of 2,6-dicyanopyridine (3.0 g, 23.0 mmol) in a mixture of Et_3N (1 cm^3) and ethanol (20 cm^3). Filtration of the precipitate gave pure pyridine-2,6-di(thioamide) as a yellow solid. Yield: 3.44 g, 75%. EI-MS: *m*/*z* 197 (50%, M^+). ^{1}H NMR [300 MHz, $(CD_3)_2SO$]: δ 10.50 (2H, s, NH), 10.26 (2H, s, NH), 8.75 (2H, d, py), 8.13 (1H, t, py). Found: C, 42.4; H, 3.4; N, 21.0%; $C_7H_7N_3S_2$ requires C, 42.6; H, 3.6; N, 21.3%.

Preparation of ligands L^1–L^4

L^1. To a solution of pyridine-2-thioamide (0.30 g, 2.17 mmol) in methanol (15 cm^3) a solution of 1,4-dibromobutane-2,3-dione (0.26 g, 1.06 mmol) in methanol (15 cm^3) was added and the solution refluxed for 1 h. After this time the resulting yellow precipitate was filtered, washed with ethanol (5 cm^3) and Et_2O (5 cm^3) and dried *in vacuo* to give L^1·2HBr. Yield: 0.41 g, 80%. Found: C, 39.8; H, 2.0; N, 10.9%; $C_{16}H_{12}N_4S_2Br_2$ requires C, 39.7; H, 2.5; N, 11.6%.

The free base ligand L^1 was prepared from the hydrobromide salt as follows. L^1·2HBr (0.20 g, 0.41 mmol) was suspended in ammonia (0.88 S.G., 50 cm^3) and left to stand for 12 h. During this time the suspension changed colour from yellow to pink. Filtration and washing with methanol (2 cm^3) and Et_2O (2 cm^3) gave L^1 as a pale pink solid. Yield: 0.13 g, 100%. EI-MS: *m*/*z* 322 (75%, M^+). ^{1}H NMR [300 MHz, $(CD_3)_2SO$]: δ 8.68 (2H, d, pyridyl), 8.26 (2H, d, py), 8.24 (2H, s, th), 8.23 (2H, t, py), 7.55 (2H, t, py) (py denotes the pyridyl group; th denotes the thiazolyl group). Found: C, 59.5; H, 2.8; N, 16.9%; $C_{16}H_{10}N_4S_2$ requires C, 59.6; H, 3.1; N, 17.4%. L^1 can be recrystallised from MeCN to give colourless plates, but the ligand was generally sufficiently pure to use directly for the complexation reactions.

L^2. To a solution of 1,10-phenanthroline-2-thioamide (0.49 g, 2.05 mmol) in methanol (25 cm^3) a solution of 1,4-dibromobutane-2,3-dione (0.25 g, 1.0 mmol) in methanol (5 cm^3) was added and the resulting solution heated at reflux for 2 h. During this time the colour changed from brown to green, and a green solid separated. Filtration and washing with methanol (2 cm^3) and Et_2O (2 cm^3) gave L^2·2HBr as a green solid. Found: C, 52.6; H, 2.4; N, 12.7%; $C_{30}H_{18}N_6S_2Br_2$ requires C, 52.5; H, 2.6; N, 12.2%. ^{1}H NMR [300 MHz, $(CD_3)_2SO$]: δ 9.38 (2H, d, phen), 9.20 (2H, d, phen), 8.89 (2H, d, phen), 8.86 (2H, d, phen), 8.55 (2H, s, th), 8.30 (6H, m, phen).

The free base ligand L^2 was prepared from the hydrobromide salt exactly as above for L^1 in quantitative yield. Analytical samples were recrystallised from hot dmso, but the ligand was generally sufficiently pure to use directly for the complexation reactions. EI-MS: *m*/*z* 524 (80%, M^+). Found: C, 60.8; H, 3.6; N, 12.8%; $C_{30}H_{16}N_6S_2$·2(Me_2SO) requires C, 60.0; H, 4.1; N, 12.3%. A ^{1}H NMR spectrum could not be obtained due to the poor solubility of the compound in common organic solvents.

L^3. To a solution of pyridine-2,6-di(thioamide) (0.30 g, 1.5 mmol) in methanol (15 cm^3) a solution of 2-(α-bromoacetyl)-pyridinium hydrobromide (1.12 g, 4.0 mmol) in methanol (15 cm^3) was added and the solution refluxed for 4 h. After this time the resulting yellow precipitate was filtered, washed with ethanol (5 cm^3) and Et_2O (5 cm^3) and dried *in vacuo* to give L^3·2HBr. The resulting hydrobromide salt was suspended in ammonia (0.88 S.G., 50 cm^3) and left to stand for 12 h. Filtration and washing with methanol (2 cm^3) and Et_2O (2 cm^3)

gave L^3 as a pale yellow solid. Yield: 0.42 g, 70%. EI-MS: *m*/*z* 399 (70%, M^+). ^{1}H NMR [300 MHz, $(CD_3)_2SO$]: δ 8.71 (2H, m, py), 8.50 (2H, s, th), 8.47 (4H, m, py), 8.28 (3H, m, py), 7.68 (2H, m, py). Found: C, 62.7; H, 3.2; N, 17.2%; $C_{21}H_{13}N_5S_2$ requires C, 63.1; H, 3.3; N, 17.5%.

L^4. To a suspension of 2,2′-bipyridine-6,6′-di(thioamide) (0.20 g, 0.73 mmol) in methanol (15 cm^3) a solution of 2-(α-bromoacetyl)pyridinium hydrobromide (0.61 g, 2.19 mmol) in methanol (15 cm^3) was added and the solution refluxed for 4 h. After this time the resulting yellow precipitate was filtered, washed with ethanol (5 cm^3) and Et_2O (5 cm^3) and dried *in vacuo* to give L^4·2HBr. This hydrobromide salt was suspended in ammonia (0.88 S.G., 50 cm^3) and left to stand for 12 h. Filtration and washing with methanol (2 cm^3) and Et_2O (2 cm^3) gave L^4 as a pale yellow solid. Yield: 0.28 g, 82%. EI-MS: *m*/*z* 476 (50%, M^+). ^{1}H NMR [300 MHz, $(CD_3)_2SO$]: δ 8.72 (2H, m, py), 8.61 (2H, d, py), 8.58 (2H, s, th), 8.40 (2H, d, py), 8.35 (2H, d, py), 8.28 (2H, t, py), 8.10 (2H, m, py), 7.54 (2H, m, py). Found: C, 66.0; H, 3.2; N, 17.1%; $C_{26}H_{16}N_6S_2$ requires C, 65.5; H, 3.4; N, 17.6%. A similar synthesis of L^4 has already been published.[12]

Preparation of metal complexes

CAUTION: perchlorate salts are potentially explosive and should be treated with due care. Those complexes described below which were isolated as perchlorates were only prepared in small amounts (10–20 mg) and we had no problems with them.

$[Cu_2(L^1)_3](PF_6)_4$. To a suspension of L^1 (0.010 g, 0.03 mmol) in acetone (2 cm^3), $Cu(PF_6)_2·6H_2O$ (0.009 g, 0.02 mmol) was added and the suspension stirred until dissolution was complete. Filtration followed by slow vapour diffusion of ethyl acetate into the solution gave $[Cu_2(L^1)_3](PF_6)_4$ as large green crystals. Yield: 0.010 g, 59%. ES-MS: *m*/*z* 1401 $[Cu_2(L^1)_3(PF_6)_2(HO)]^+$. Found: C, 33.7; H, 2.0; N, 10.0%; $C_{48}H_{30}N_{12}S_6Cu_2P_4F_{24}$ requires C, 33.9; H, 1.9; N, 10.5%.

$[Zn_2(L^1)_3](ClO_4)_4$. To a suspension of L^1 (0.010 g, 0.03 mmol) in nitromethane (2 cm^3) $Zn(ClO_4)_2·6H_2O$ (0.008 g, 0.02 mmol) was added and the solution stirred until dissolution was complete. Filtration followed by slow vapour diffusion of ethyl acetate into the solution gave $[Zn_2(L^1)_3](ClO_4)_4$ as large colourless crystals. Yield: 0.007 g, 50%. ^{1}H NMR (300 MHz, CD_3NO_2): δ 8.27 (12H, m, py), 7.97 (dt, 6H, py, J = 5.1, 1.1 Hz), 7.59 (6H, m, py), 7.52 (6H, s, th). ES-MS: *m*/*z* 1396 $[Zn_2(L^1)_3(ClO_4)_3]^+$, 648 $[Zn_2(L^1)_3(ClO_4)_2]^{2+}$. Found: C, 37.7; H, 2.0; N, 10.6%; $C_{48}H_{30}N_{12}S_6Zn_2Cl_4O_{16}$ requires C, 38.5; H, 2.0; N, 11.2%.

$[Co_2(L^1)_3](ClO_4)_4$. This was prepared (as orange crystals) from L^1 and $Co(ClO_4)_2·6H_2O$ in exactly the same way as for the Zn(II) analogue above. Yield: 0.01 g, 70%. ES-MS: *m*/*z* 1383 $[Co_2(L^1)_3(ClO_4)_3]^+$, 642 $[Co_2(L^1)_3(ClO_4)_2]^{2+}$. Found: C, 37.9; H, 2.0; N, 10.9%; $C_{48}H_{30}N_{12}S_6Co_2Cl_4O_{16}$ requires C, 38.9; H, 2.0; N, 11.3%.

$[Cu_2(L^2)_2](ClO_4)_4$. To a suspension of L^2 (0.010 g, 0.019 mmol) in nitromethane (2 cm^3) $Cu(ClO_4)_2·6H_2O$ (0.007 g, 0.019 mmol) was added and the solution stirred until dissolution was complete. Filtration followed by slow vapour diffusion of ethyl acetate into the solution gave $[Cu_2(L^2)_2](ClO_4)_4$ as green crystals. Yield: 0.007 g, 51%. ES-MS: *m*/*z* 1473 $[Cu_2(L^2)_2(ClO_4)_3]^+$, 686 $[Cu_2(L^2)_2(ClO_4)_2]^{2+}$. Found: C, 46.4; H, 2.1; N, 10.2%; $C_{60}H_{32}N_{12}S_4Cu_2Cl_4O_{16}$ requires C, 45.8; H, 2.0; N, 10.7%.

$[Zn_2(L^2)_2](ClO_4)_4$. This was prepared from L^2 (0.010 g, 0.019 mmol) and $Zn(ClO_4)_2·6H_2O$ (0.007 g, 0.019 mmol) in exactly the same way as for the Cu(II) analogue above. Yield: 0.010 g, 67%. ^{1}H NMR (300 MHz, CD_3NO_2): δ 9.35 (d, 4H, phen, J = 8.5), 8.90 (d, 4H, phen, J = 8.5), 8.53 (dd, 4H, phen, J = 8.3, 1.4), 8.39 (d, 4H, phen, J = 9.1), 8.23 (d, 4H, phen, J = 9.1), 7.68 (dd, 4H, phen, J = 4.8, 1.4), 7.50 (dd, 4H, phen, J = 8.3, 4.8 Hz), 7.20 (s, 4H, th). ES-MS: *m*/*z* 1476 $[Zn_2(L^2)_2(ClO_4)_3]^+$, 687 $[Zn_2(L^2)_2(ClO_4)_2]^{2+}$. Found: C, 45.6; H, 2.0; N, 10.7%; $C_{60}H_{32}N_{12}S_4Zn_2Cl_4O_{16}$ requires C, 45.7; H, 2.0; N, 10.6%.

$[Cu_2(L^3)_2](ClO_4)_4$. To a suspension of L^3 (0.010 g, 0.025 mmol) in nitromethane (2 cm^3) $Cu(ClO_4)_2·6H_2O$ (0.009 g, 0.02 mmol) was added and the solution stirred until dissolution was complete. Filtration followed by slow vapour diffusion of ethyl acetate into the solution gave $[Cu_2(L^3)_2](ClO_4)_4$ as large green crystals. Yield: 0.010 g, 61%. ES-MS: *m*/*z* 1224 $[Cu_2(L^3)_2(ClO_4)_3]^+$, 562 $[Cu_2(L^3)_2(ClO_4)_2]^{2+}$. Found: C, 37.5; H, 2.1; N, 10.0%; $C_{42}H_{26}N_{10}S_4Cu_2Cl_4O_{16}$ requires C, 38.1; H, 2.0; N, 10.6%.

$[Cu_2(L^4)_2](ClO_4)_4$. To a suspension of L^4 (0.010 g, 0.021 mmol) in nitromethane (2 cm^3) $Cu(ClO_4)_2·6H_2O$ (0.007 g, 0.02 mmol) was added and the solution stirred until dissolution was complete. Filtration followed by slow vapour diffusion of ethyl acetate into the solution gave $[Cu_2(L^4)_2](ClO_4)_4$ as large green crystals. Yield: 0.006 g, 41%. ES-MS: *m*/*z* 1378 $[Cu_2(L^4)_2(ClO_4)_3]^+$, 639 $[Cu_2(L^4)_2(ClO_4)_2]^{2+}$. Found: C, 42.0; H, 2.0; N, 10.9%; $C_{52}H_{32}N_{12}S_4Cu_2Cl_4O_{16}$ requires C, 42.2; H, 2.2; N, 11.4%.

X-Ray crystallography

Diffraction intensity data were collected on a Siemens SMART-CCD diffractometer. The software used was SHELXS-97 for structure solution;[23] SHELXL-97 for structure refinement;[23] and SADABS for the absorption correction.[24] Details of the crystal parameters, data collection and refinement are collected in Table 1, and selected metric parameters are in Tables 2–5.

CCDC reference number 186/2325.

See http://www.rsc.org/suppdata/dt/b0/b007922g/ for crystallographic files in .cif format.

The structural determinations of the metal complexes tended to be complicated by a combination of extensive solvation, which resulted in poor crystallinity and weak data, and disorder in the counter-ions and solvent molecules which could not always be resolved. For $[Zn_2(L^2)_2][ClO_4]_4·9MeCN$ the data were very weak and it was only possible to refine the structure with isotropic thermal parameters throughout; the esd's on the structural parameters for this complex are high and accordingly the structure should be regarded only as confirming the gross helical architecture of the complex. In each member of the isostructural series $[Cu_2(L^1)_3][PF_6]_4·4Me_2CO$, $[Zn_2(L^1)_3][ClO_4]_4·4MeNO_2$ and $[Zn_2(L^1)_3][ClO_4]_4·4MeNO_2$ one of the two independent solvent molecules is well defined but the other has a highly irregular geometry with some residual electron-density peaks nearby. Attempts to force the geometry to be more regular using restraints were not successful, and attempts to model the disorder more accurately by introducing a greater number of parameters into the refinement led to the refinement becoming unstable. Similar problems were encountered with one of the solvent molecules of $[Cu_2(L^3)_2][ClO_4]_4·4MeNO_2$. A general feature of these structures is accordingly (i) high thermal parameters for some of the solvent/anion atoms, and (ii) residual electron-density peaks of up to 2 e Å^{-3} associated with the disordered solvents/anions. With this in mind the quality of the refinements is reasonable and the R_1 values we obtained (Table 1) are entirely typical of large, highly charged, and highly solvated molecules of this general type. In all cases the complex cations are clearly defined and well resolved with no disorder problems.

Table 3 Selected bond lengths (Å) and angles (°) for $[Cu_2(L^2)_2][ClO_4]_4 \cdot 8MeCN \cdot H_2O$ and $[Zn_2(L^2)_2][ClO_4]_4 \cdot 9MeCN$. Parameters which are equivalent between the two structures are listed in the same row of the table

Cu(1)–N(121)	1.972(11)	Zn(1)–N(124)	2.043(18)
Cu(1)–N(144)	1.987(11)	Zn(1)–N(141)	2.103(19)
Cu(1)–N(124)	2.111(12)	Zn(1)–N(121)	2.182(18)
Cu(1)–N(141)	2.138(13)	Zn(1)–N(144)	2.185(17)
Cu(1)–N(111)	2.226(12)	Zn(1)–N(101)	2.236(19)
Cu(1)–N(101)	2.311(13)	Zn(1)–N(111)	2.215(19)
Cu(2)–N(244)	1.965(12)	Zn(2)–N(221)	2.056(19)
Cu(2)–N(221)	1.968(12)	Zn(2)–N(244)	2.043(19)
Cu(2)–N(241)	2.129(14)	Zn(2)–N(224)	2.199(18)
Cu(2)–N(224)	2.148(11)	Zn(2)–N(241)	2.204(17)
Cu(2)–N(201)	2.258(12)	Zn(2)–N(201)	2.184(17)
Cu(2)–N(211)	2.299(13)	Zn(2)–N(211)	2.249(17)
N(121)–Cu(1)–N(144)	173.9(5)	N(124)–Zn(1)–N(141)	170.1(7)
N(121)–Cu(1)–N(124)	79.3(5)	N(124)–Zn(1)–N(121)	74.6(7)
N(144)–Cu(1)–N(124)	95.6(5)	N(141)–Zn(1)–N(121)	97.8(7)
N(121)–Cu(1)–N(141)	98.7(5)	N(124)–Zn(1)–N(144)	98.3(7)
N(144)–Cu(1)–N(141)	79.2(5)	N(141)–Zn(1)–N(144)	76.6(7)
N(124)–Cu(1)–N(141)	102.1(5)	N(121)–Zn(1)–N(144)	100.9(6)
N(121)–Cu(1)–N(111)	76.3(5)	N(124)–Zn(1)–N(101)	74.7(7)
N(144)–Cu(1)–N(111)	109.3(5)	N(141)–Zn(1)–N(101)	113.6(7)
N(124)–Cu(1)–N(111)	154.1(4)	N(121)–Zn(1)–N(101)	148.1(7)
N(141)–Cu(1)–N(111)	90.0(4)	N(144)–Zn(1)–N(101)	91.9(7)
N(121)–Cu(1)–N(101)	108.7(5)	N(124)–Zn(1)–N(111)	112.5(7)
N(144)–Cu(1)–N(101)	74.3(5)	N(141)–Zn(1)–N(111)	73.4(7)
N(124)–Cu(1)–N(101)	91.1(5)	N(121)–Zn(1)–N(111)	90.5(7)
N(141)–Cu(1)–N(101)	151.4(4)	N(144)–Zn(1)–N(111)	149.1(7)
N(111)–Cu(1)–N(101)	88.8(4)	N(111)–Zn(1)–N(101)	93.2(7)
N(244)–Cu(2)–N(221)	173.6(5)	N(244)–Zn(2)–N(221)	169.0(7)
N(244)–Cu(2)–N(241)	79.5(5)	N(221)–Zn(2)–N(224)	76.1(7)
N(221)–Cu(2)–N(241)	98.2(5)	N(244)–Zn(2)–N(224)	96.8(7)
N(244)–Cu(2)–N(224)	96.3(5)	N(221)–Zn(2)–N(241)	95.9(7)
N(221)–Cu(2)–N(224)	78.4(5)	N(244)–Zn(2)–N(241)	77.0(7)
N(241)–Cu(2)–N(224)	105.3(5)	N(224)–Zn(2)–N(241)	101.1(6)
N(244)–Cu(2)–N(201)	110.7(5)	N(221)–Zn(2)–N(201)	114.8(7)
N(221)–Cu(2)–N(201)	75.2(5)	N(244)–Zn(2)–N(201)	73.3(7)
N(241)–Cu(2)–N(201)	88.8(5)	N(201)–Zn(2)–N(224)	91.7(7)
N(224)–Cu(2)–N(201)	151.6(5)	N(201)–Zn(2)–N(241)	148.8(7)
N(244)–Cu(2)–N(211)	74.7(5)	N(221)–Zn(2)–N(211)	73.6(7)
N(221)–Cu(2)–N(211)	108.6(5)	N(244)–Zn(2)–N(211)	114.2(7)
N(241)–Cu(2)–N(211)	151.6(5)	N(224)–Zn(2)–N(211)	148.9(7)
N(224)–Cu(2)–N(211)	89.3(4)	N(241)–Zn(2)–N(211)	88.9(6)
N(201)–Cu(2)–N(211)	89.3(4)	N(201)–Zn(2)–N(211)	94.6(6)

Table 4 Selected bond lengths (Å) and angles (°) for $[Cu_2(L^3)_2][ClO_4]_4 \cdot 4MeNO_2$

Cu(1)–N(121)	1.956(5)	Cu(2)–N(251)	1.971(5)
Cu(1)–N(221)	1.969(5)	Cu(2)–N(151)	1.983(5)
Cu(1)–N(211)	2.007(5)	Cu(2)–N(241)	2.016(5)
Cu(1)–N(111)	2.014(5)	Cu(2)–N(141)	2.071(5)
N(121)–Cu(1)–N(221)	159.6(2)	N(251)–Cu(2)–N(151)	161.7(2)
N(121)–Cu(1)–N(211)	104.0(2)	N(251)–Cu(2)–N(241)	81.5(2)
N(221)–Cu(1)–N(211)	81.9(2)	N(151)–Cu(2)–N(241)	103.8(2)
N(121)–Cu(1)–N(111)	81.6(2)	N(251)–Cu(2)–N(141)	107.0(2)
N(221)–Cu(1)–N(111)	106.3(2)	N(151)–Cu(2)–N(141)	81.1(2)
N(211)–Cu(1)–N(111)	141.2(2)	N(241)–Cu(2)–N(141)	137.5(2)

Table 5 Selected bond lengths (Å) and angles (°) for $[Cu_2(L^4)_2][ClO_4]_4 \cdot 2MeNO_2$

Cu(1)–N(111)	1.923(4)	Cu(2)–N(211)	1.925(4)
Cu(1)–N(101)	1.928(4)	Cu(2)–N(201)	1.930(4)
Cu(1)–N(121)	2.097(3)	Cu(2)–N(221)	2.103(4)
Cu(1)–N(131)	2.134(4)	Cu(2)–N(231)	2.136(4)
N(111)–Cu(1)–N(101)	173.87(16)	N(211)–Cu(2)–N(201)	173.36(15)
N(111)–Cu(1)–N(121)	79.81(14)	N(211)–Cu(2)–N(221)	79.24(15)
N(101)–Cu(1)–N(121)	101.47(15)	N(201)–Cu(2)–N(221)	101.55(15)
N(111)–Cu(1)–N(131)	104.86(15)	N(211)–Cu(2)–N(231)	106.15(15)
N(101)–Cu(1)–N(131)	79.62(15)	N(201)–Cu(2)–N(231)	79.05(15)
N(121)–Cu(1)–N(131)	122.29(14)	N(221)–Cu(2)–N(231)	123.09(14)

Acknowledgements

We thank the University of Huddersfield, the EPSRC, and the Leverhulme foundation for financial support. We would also like to thank Dr John Maher (University of Bristol) for recording the EPR spectra.

References

1 C. Piguet, G. Bernardinelli and G. Hopfgartner, *Chem. Rev.*, 1997, **97**, 2005; E. C. Constable, in *Polynuclear Transition Metal Helicates, vol. 9, Comprehensive Supramolecular Chemistry*, editor: J.-P. Sauvage, Elsevier, Oxford, 1996, pp. 213–252.

2 M. Albrecht, *Chem. Soc. Rev.*, 1998, **27**, 281; M. Albrecht, O. Blau and H. Röttele, *New J. Chem.*, 2000, **24**, 619.

3 M. Elhabiri, R. Scopelliti, J.-C. G. Bunzli and C. Piguet, *J. Am. Chem. Soc.*, 1999, **121**, 10747; S. Rigault, C. Piguet and J.-C. G. Bünzli, *J. Chem. Soc., Dalton Trans.*, 2000, 2045; C. Piguet, *J. Incl. Phenom. Macrocycl. Chem.*, 1999, **34**, 361.

4 R. Stiller and J.-M. Lehn, *Eur. J. Inorg. Chem.*, 1998, 977; B. Hasenknopf, J.-M. Lehn, N. Boumediene, E. Leize and A. van Dorsselaer, *Angew. Chem., Int. Ed.*, 1998, **37**, 3265.

5 J. S. Fleming, E. Psillakis, S. M. Couchman, J. C. Jeffery, J. A. McCleverty and M. D. Ward, *J. Chem. Soc., Dalton Trans.*, 1998, 537; M. J. Hannon, S. Bunce, A. J. Clarke and N. W. Alcock, *Angew. Chem., Int. Ed.*, 1999, **38**, 1277; N. K. Solanki, A. E. H. Wheatley, S. Radojevic, M. McPartlin and M. A. Halcrow, *J. Chem. Soc., Dalton Trans.*, 1999, 521; O. Mamula, A. von Zelewsky, T. Bark and G. Bernardinelli, *Angew. Chem., Int. Ed.*, 1999, **38**, 2945; R. Ziessel, A. Harriman, A. El-Ghayoury, L. Douce, E. Leize, H. Nierengarten and A. van Dorsselaer, *New J. Chem.*, 2000, **24**, 729.

6 E. C. Constable, *Prog. Inorg. Chem.*, 1994, **42**, 67.

7 K. T. Potts, *Bull. Soc. Chim. Belg.*, 1990, **99**, 741; K. T. Potts, M. Keshavarz-K, F. S. Tham, H. D. Abruña and C. Arana, *Inorg. Chem.*, 1993, **32**, 4436; K. T. Potts, M. P. Wentland, D. Ganguly, G. D. Storrier, S. K. Cha, J. Cha and H. D. Abruña, *Inorg. Chim. Acta*, 1999, **288**, 189.

8 E. C. Constable, S. M. Elder, J. Healy and D. A. Tocher, *J. Chem. Soc., Dalton Trans.*, 1990, 1669; E. C. Constable, S. M. Elder, J. Healy, M. D. Ward and D. A. Tocher, *J. Am. Chem. Soc.*, 1990, **112**, 4590.

9 E. C. Constable, S. M. Elder, M. J. Hannon, A. Martin, P. R. Raithby and D. A. Tocher, *J. Chem. Soc., Dalton Trans.*, 1996, 2423.

10 E. C. Constable, M. D. Ward and D. A. Tocher, *J. Chem. Soc., Dalton Trans.*, 1991, 1675.

11 C. R. Rice, S. Wörl, J. C. Jeffery, R. L. Paul and M. D. Ward, *Chem. Commun.*, 2000, 1529.

12 P. N. W. Baxter, J. A. Connor, W. B. Schweizer and J. D. Wallis, *J. Chem. Soc., Dalton Trans.*, 1992, 3015.

13 R. Menasse, G. Klien and H. Erlenmeyer, *Helv. Chim. Acta.*, 1955, 1289.

14 H. A. Goodwin, F. E. Smith, E. König and G. Ritter, *Aust. J. Chem.*, 1973, **26**, 521.

15 E. C. Constable, S. M. Elder, J. V. Walker, P. D. Wood and D. A. Tocher, *J. Chem. Soc., Chem. Commun.*, 1992, 229; and refs. therein; K. T. Potts, K. A. G. Rayford and M. Keshavarz-K, *J. Am. Chem. Soc.*, 1993, **115**, 2793.

16 R. E. Rosenfeld, Jr., R. Parthasarathy and J. D. Dunitz, *J. Am. Chem. Soc.*, 1977, **99**, 4860; T. N. G. Row and R. Parthasarathy, *J. Am. Chem. Soc.*, 1981, **103**, 477.

17 M. A. Leech, N. Solanki, M. A. Halcrow, J. A. K. Howard and S. Dahaoui, *Chem. Commun.*, 1999, 2245; J.-V. Folgado, W. Henke, R. Allmann, H. Stratemeier, D. Beltrán-Porter, T. Rojo and D. Reinen, *Inorg. Chem.*, 1990, **29**, 2035.

18 E. C. Constable, *Adv. Inorg. Chem. Radiochem.*, 1986, **30**, 69; B. Whittle, E. L. Horwood, L. H. Rees, S. R. Batten, J. C. Jeffery and M. D. Ward, *Polyhedron*, 1998, **17**, 373.

19 D. A. Bardwell, A. M. W. Cargill Thompson, J. C. Jeffery, E. E. M. Tilley and M. D. Ward, *J. Chem. Soc., Dalton Trans.*, 1995, 835; P. J. Burke, D. R. McMillin and W. R. Robinson, *Inorg. Chem.*, 1980, **19**, 1211; M. Geoffroy, M. Wermeille, C. O. Buchecker, J.-P. Sauvage and G. Bérnardinelli, *Inorg. Chim. Acta*, 1990, **167**, 157; M. Cesario, C. O. Dietrich-Buchecker, T. Guilhem, C. Pascard and J.-P. Sauvage, *J. Chem. Soc., Chem. Commun.*, 1985, 244; K. Klemens, C. E. A. Palmer, S. M. Rolland, P. E. Fanwick, D. R. McMillin and J.-P. Sauvage, *New J. Chem.*, 1990, **14**, 129.

20 B. J. Hathaway, in *Comprehensive Coordination Chemistry*, editors: G. Wilkinson, R. D. Gillard and J. A. McCleverty, Pergamon, 1987, vol. 5, p. 533.

21 B. J. Hathaway and D. E. Billing, *Coord. Chem. Rev.*, 1970, **5**, 143; W. Fitzgerald and B. J. Hathaway, *J. Chem. Soc., Dalton Trans.*, 1981, 567.

22 M. Albrecht, O. Blau and J. Zauner, *Eur. J. Org. Chem.*, 1999, 3165; M. Albrecht, M. Schneider and H. Röttele, *Angew. Chem., Int. Ed.*, 1999, **38**, 557; M. Albrecht, O. Blau and R. Fröhlich, *Chem. Eur. J.*, 1999, **5**, 48; M. Albrecht, O. Blau, E. Wegelius and K. Rissanen, *New J. Chem.*, 1999, **23**, 667; J. Xu, T. N. Parac and K. N. Raymond, *Angew. Chem., Int. Ed.*, 1999, **38**, 2878.

23 G. M. Sheldrick, SHELXS-97 and SHELXL-97, University of Göttingen, Göttingen, 1997.

24 G. M. Sheldrick, SADABS, A program for absorption correction with the Siemens SMART area-detector system, University of Göttingen, Göttingen, 1996.